Progress In Electromagnetics Research Letters, Vol. 66, 53–58, 2017

A Frequency Reconfigurable Dual Pole Dual Band Bandpass Filter for X-Band Applications

Amit Bage* **and Sushrut Das**

Abstract—This paper presents a frequency reconfigurable dual-pole, dual-band waveguide bandpass filter. Varactor diode and chip capacitor loaded planar split ring resonators are placed on the transverse plane of a waveguide to form the filter. Numerical simulations are carried out using CST microwave studio (version 14). Measured tuning ranges of the bands are 8.12–8.58 GHz and 10.22–10.68 GHz, respectively. Measured result shows good agreement with the simulated one. The total length of the filter is 10 mm.

1. INTRODUCTION

Compact, light weight, frequency reconfigurable, multiband waveguide bandpass filters find numerous applications in present day wireless communication systems. To reduce the volume and weight of waveguide filters, printed circuit inserts are often used on the E-plane/transverse plane of a waveguide [1–4]. For tuning the operating frequency, several mechanisms, such as magnetic tuning [5], varactor loaded frequency selective surface [6–8], micro-electromechanical system [9, 10], E-plane varactor [11], optical tuning [12–14], liquid metal posts [15], are used. Following the requirements of multiband filters, several multiband waveguide filters have also been proposed [16–20]. However, none of these filters simultaneously fulfills all the above filter characteristics (i.e., compactness, light weight, frequency reconfigurability and multiple operating band). Therefore, an attempt is made in this work to design a compact, light weight, frequency reconfigurable, dual-band waveguide bandpass filter using varactor diode and chip capacitor loaded planar split ring resonator inserts. Two independent sets of varactor bias voltages are used to independently control the center frequencies of the two bands. The filter is 10 mm long which makes the filter compact and light weight.

2. FILTER GEOMETRY AND ANALYSIS

The proposed planar insert is shown in Fig. 1, and its placement inside the waveguide (WR-90) is shown in Fig. 2. The insert is printed on a Roger RO 4350 dielectric substrate of relative dielectric constant (ε_r) 3.66, loss tangent (δ) 0.004, slab thickness 0.762 mm and copper thickness 0.035 mm. Equivalent circuit of the structure (Fig. 2) can be represented by two parallel LC resonators and coupling inductances and capacitances between them. The parallel resonators represent the CSRRs, and the coupling inductances and capacitances represent the coupling between them. Presence of the coupling inductances and capacitances makes the equivalent circuit complicated and difficult to analyze. Therefore, for analysis purpose weak coupling case is assumed which neglects the coupling inductances and capacitances and thus simplifies the structure. An equivalent LC network of the structure (Fig. 2), under weak coupling and lossless case, is shown in Fig. 3. To validate the circuit model (Fig. 3) and weak coupling approximation, simulated frequency responses of both the structures (Fig. 2 and Fig. 3)

Received 5 January 2017, Accepted 8 February 2017, Scheduled 21 February 2017

* Corresponding author: Amit Bage (bageism@gmail.com).
The authors are with the Department of Electronics Engineering, Indian Institute of Technology (Indian School of Mines), Dhanbad, Jharkhand 826004, India.

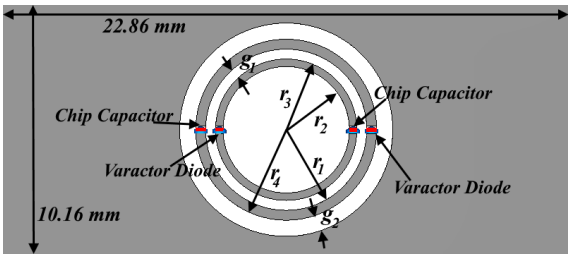

Figure 1. Proposed planar insert.

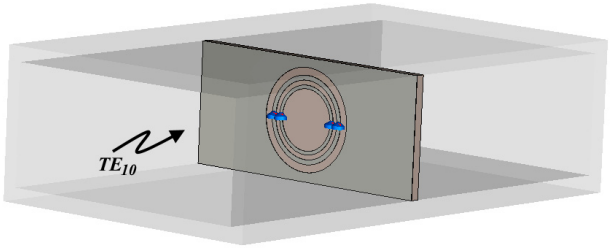

Figure 2. Placement of the insert inside a WR-90 waveguide.

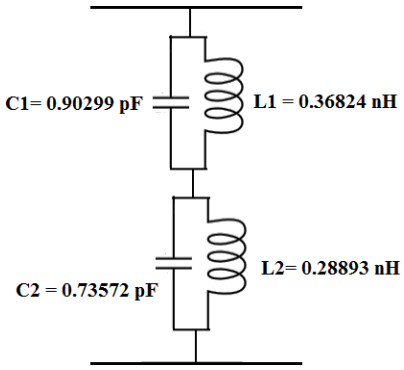

Figure 3. Lumped element equivalent circuit of the Fig. 2 (under weak coupling and lossless case).

are plotted and compared in Fig. 4. The figure reveals a reasonable agreement between them. Values of the equivalent L and C of the proposed dual-band resonator can be calculated from frequency response of the structure in Fig. 2 using the relations [20]:

$$L_{eq} = \frac{5B_{3\,\mathrm{dBi}}Z_{0i}\,|S_{21}\,(j\omega_{0i})|}{(\omega_{0i})^2} \tag{1}$$

$$C_{eq} = \frac{0.2}{B_{3\,\mathrm{dBi}}Z_{0i}\,|S_{21}\,(j\omega_{0i})|} \tag{2}$$

where $B_{3\,\mathrm{dBi}}$, Z_{0i} and $S_{21}(j\omega_{0i})$ are 3 dB bandwidth, characteristics impedance and insertion loss at the respective bands. Equations (1) and (2) assumes a 500 Ohm characteristic impedance system.

If the bias voltages are changed, the capacitances of the varactor diodes are also changed, which in turn, changes the overall capacitance of the system and hence the resonance frequency of the LC resonator. The variation of the resonance frequency of the LC resonator with variation of the capacitance value (or bias voltage) is shown in Fig. 5. To plot the graph, the dimensions of the SRRs are assumed as $r_1 = 3.25$, $r_2 = 2.35$, $r_3 = 2.85$, $r_4 = 3.6$, $g_1 = 0.4$, $g_2 = 0.65$ (all in mm). The value of the chip capacitor is kept fixed at 120 pF.

Once the unit cell is characterized, next task is to design a dual-band dual-pole bandpass filter. To insert another pole, two identical planar inserts are placed at a distance "l", as shown in Fig. 6. In the figure, "h" indicates the thickness of the dielectric and copper cladding of the substrate. To analyse the coupling between the identical inserts and its effect on the frequency response of the filter, parametric analysis of the structure is carried out for different values of "l". The result is shown in Fig. 7. It reveals that an acceptable frequency response can be achieved for $l = 8.41$ mm. It may be noted that this separation is approximately quarter wavelength long at the center of X-band (10 GHz). For TE_{10} mode at 10 GHz, the guided wavelength of the propagating wave in dielectric (Roger RO4350 substrate) and air filled regions are 16.99 and 39.76 mm, respectively. Therefore, the dielectric and air filled regions are 16.10° and 76.15° long, and the total separation between the planar inserts is 92.15°.

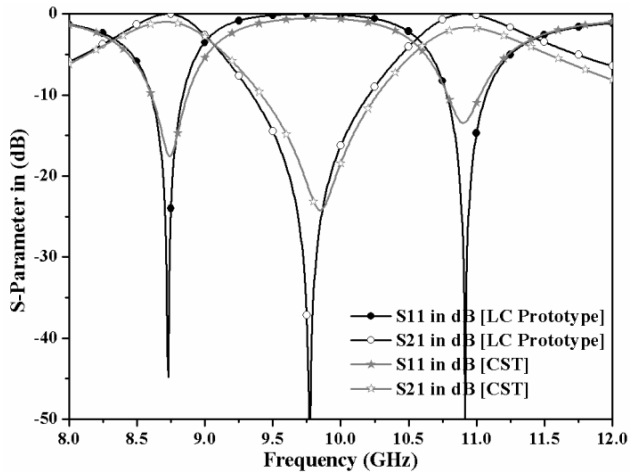

Figure 4. Comparison of the frequency responses (magnitude of S-parameters) of the structure in Fig. 2 and its equivalent circuit in Fig. 3.

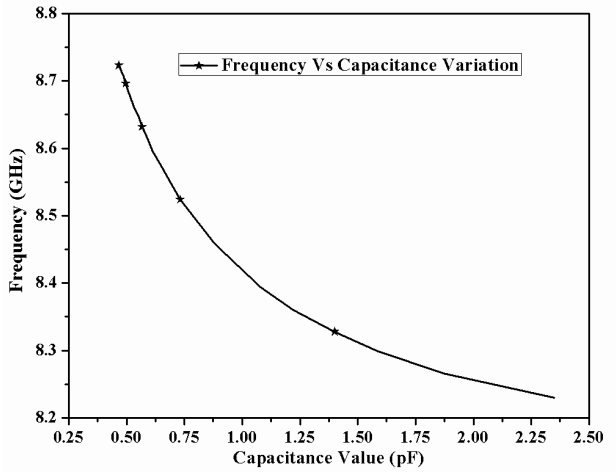

Figure 5. Variation of resonance frequency with capacitance of the varactor.

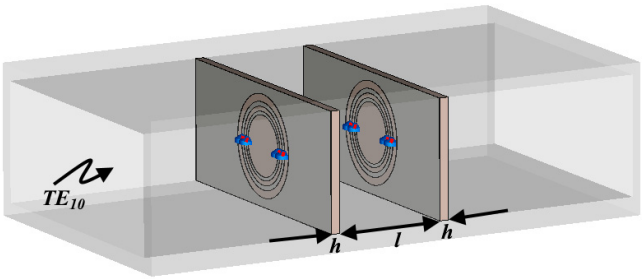

Figure 6. 3D model of the proposed filter.

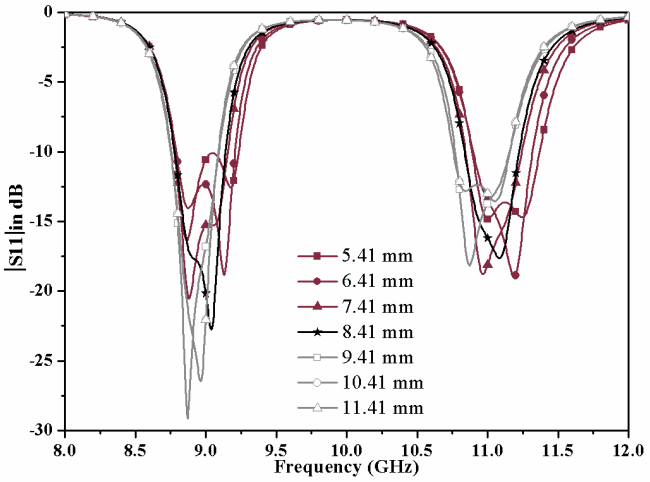

Figure 7. Parametric analysis of the structure for different lengths (l).

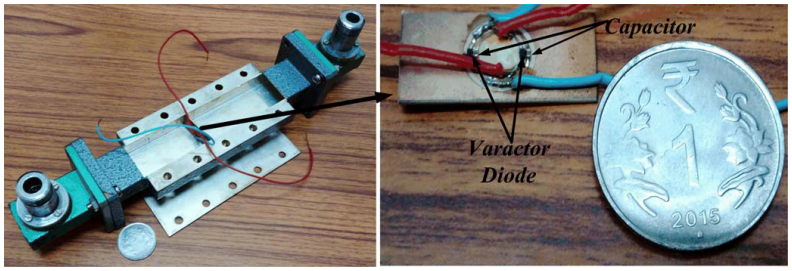

Figure 8. Fabricated unit cell and its placement inside WR-90 waveguide.

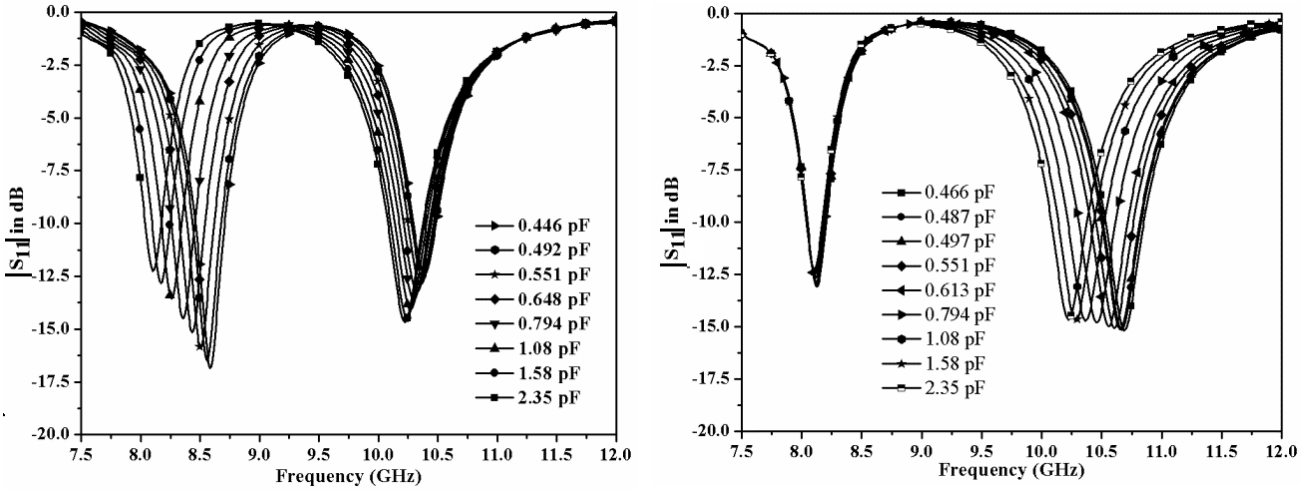

Figure 9. Measured unit cell responses for different biasing voltage (a) for first band and (b) for second band.

3. RESULT AND DISCUSSION

The fabricated planar insert and its placement inside a WR-90 waveguide are shown in Fig. 8. Skyworks SMV1231 varactor is used for fabrication purpose. In the biasing circuits, a 2 µH RF chock coil (EPCOS/TDK) is used in series with 1 kΩ resistance to prevent any RF leakage to the DC supply. The fixed capacitor (120 pF) acts as a DC blocking capacitor. Since the biasing lines are conductors, they may disturb the field distribution in the waveguide. Therefore, in the proposed work the biasing lines are routed in such a way that its major part passes through a low-field region (such as along the walls of the waveguide where electric field is very weak). This minimizes the disturbance.

Measurements of the scattering parameters are carried out using a calibrated Keysight PNA vector network analyzer (Model No. N5221A). Measured unit cell (Fig. 2) $|S_{11}|$ responses for different biasing voltages (and hence varactor capacitances) are shown in Fig. 9. The figure reveals that by varying the varactor capacitances individual bands can be frequency reconfigured. The tuning bandwidths of the lower and upper bands are 475 and 465 MHz, respectively.

Simulated and measured S-parameter responses (magnitude) of the filter (Fig. 6) for different biasing voltages are shown in Fig. 10. The figure reveals a reasonable agreement between them. The slight mismatches are due to the presence of parasitic soldering capacitances and biasing wires. The figure also reveals that as the bias voltages are increased, the varactor provides lower capacitance and shifts the bands towards higher frequencies. Therefore, by adjusting the bias voltages, the desired center frequencies can be achieved.

A comparison of the proposed filter with a few other reported reconfigurable waveguide filters [16–18] is given Table 1. It shows that the proposed filter is compact compared to others.

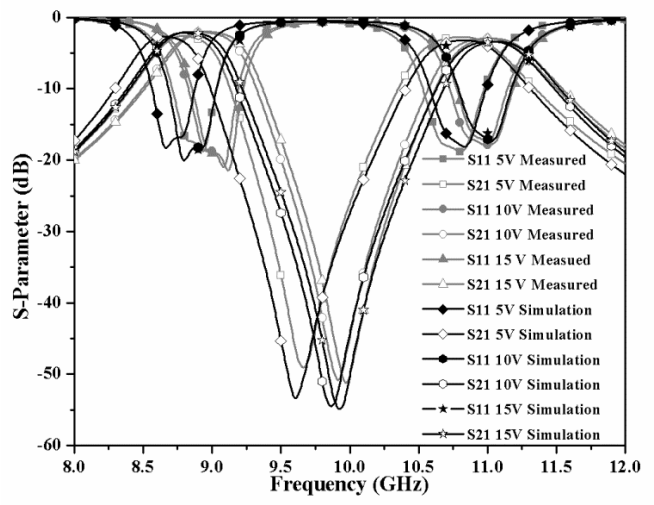

Figure 10. Comparison of the simulated and measured S-parameters (magnitude) of the filter for different biasing voltages.

Table 1. Comparison of the proposed filter with few other reconfigurable waveguide bandpass filter.

Reference	Tuning Range in (GHz)	Mode of Tuning	Loaded and Unloaded Quality Factor	Electrical Length
[11] [Simulated]	9.405–9.685	Varactor	21.68/86.68	$1.3867\lambda_g$
[12] [Measured]	9.25–9.7	Graphine	18.49/86.094	$0.2416\lambda_g$
[13] [Measured]	10.8–11.3	Silicon Doped	48/179.65	$1.2523\lambda_g$
Proposed Work	8.2–8.7/ 10.2–10.9	Varactor Diode	19.28/74.77 and 17.09/62.99	$0.1775\lambda_g$

The loaded and unloaded quality factors can be calculated using the relations:

$$Q_L = \frac{f_0}{(\Delta f)_{3\,\mathrm{dB}}} \tag{3}$$

$$Q_U = \frac{Q_L}{\left(1 - 10^{-IL/20}\right)} \tag{4}$$

where f_0, $(\Delta f)_{3\,\mathrm{dB}}$, and IL are the resonant frequency, 3-dB bandwidth and insertion loss, respectively. After substituting the values, the loaded and unloaded quality factors for the first and second bands are found to be 19.28, 17.09 and 74.77, 62.99, respectively.

4. CONCLUSION

This paper presents a compact, frequency reconfigurable, dual-pole, dual-band waveguide bandpass filter. The dual bands are achieved by loading split ring resonators with chip capacitors and varactor diodes. Dual poles are achieved by placing two identical inserts at an optimized distance of 8.41 mm. Tuning of the center frequencies of each band can be achieved by varying the capacitance (or biasing voltage) of the respective varactor diode. Tuning ratios of 5.69% and 4.45% are achieved for the first and second bands, respectively. Measured insertion losses at both the bands are 2.59 and 2.75 dB, respectively. The loaded and unloaded quality factors for the first and second bands are 19.28/17.09 and 74.77/62.99, respectively. The length of the filter is 10 mm, which makes it compact and light weight.

REFERENCES

1. Bage, A. and S. Das, "A compact, wideband waveguide bandpass filter using complementary loaded split ring resonators," *Progress In Electromagnetics Research C*, Vol. 64, 51–59, 2016.
2. Bage, A. and S. Das, "Wideband waveguide band-pass filter based on broadside complementary split ring resonator," *Int. Conf. Microw. and Photonics (ICMAP)*, 1–2, 2015.
3. Jin, J. Y., X. Q. Lin, Y. Jiang, L. Wang, and Y. Fan, "A novel E-plane substrate inserted bandpass filter with high selectivity and compact size," *Int. Journal of RF Microw. Comput. Aided Eng.*, Vol. 17, 451–456, 2007.
4. Jin, J. Y., X. Q. Lin, Y. Jiang, and Q. Xue, "A novel compact-plane waveguide filter with multiple transmission zeroes," *IEEE Trans. Microw. Theory Tech.*, Vol. 63, No. 10, 3374–3380, 2015.
5. Bernardi, P. and F. Valdoni, "Fundamentals of a new class of magnetically tunable waveguide filters," *IEEE Trans. on Magnetics*, Vol. 2, No. 3, 264–268, 1966.
6. Mias, C., "Waveguide and free-space demonstration of tunable frequency selective surface," *Electro. Lett.*, Vol. 39, 850–852, 2003.
7. Mias, C., "Demonstration of wideband tuning of frequency selective surface in waveguide setup," *Microw. Opt. Technol. Lett.*, Vol. 44, 412–416, 2005.
8. Tsakonas, C. and C. Mias, "Electrically-tunable band-stop filter with mechanically variable bandwidth," *Microw. Opt. Technol. Lett.*, Vol. 48, 53–56, 2006.
9. Pelliccia, L., S. Bastioli, F. Casini, and R. Sorrentino, "High-Q MEMS-reconfigurable waveguide filters," *Proceedings of the 40th European Microw. Conf.*, 1126–1129, 2010.
10. Pelliccia, L., S. Bastioli, F. Casini, and R. Sorrentino, "High Q tunable waveguide filters using ohmic RF MEMS switches," *IEEE Trans. Microw. Theory Techniques*, Vol. 63, No. 10, 3381–3390, 2015.
11. Mohottige, N., U. Jankovic, D. Budimir, and U. Jankovic, "Compact E-plane varactor-tuned bandpass filters," *Antennas and Propag. Society Int. Symp. (APSURSI)*, 790–791, 2013.
12. Mohottige, N., B. Bukvic, and D. Budimir, "Reconfigurable E-plane waveguide resonators for filter applications," *44th European Microw. Conf., (EuMC)*, 299–301, 2014.
13. Mohottige, N., D. Budimir, and C. J. Panagamuwa, "Optically reconfigurable E-plane waveguide resonators and filters," *43rd European Microw. Conf.*, 798–801, 2013.
14. Zhang, M., P. Ye, F. Zhang, Y. Zhao, and J. Wang, "NOLM-based wavelength conversion with FBG band-pass filter for optical packet switching," *Chin. Opt. Lett.*, Vol. 1, No. 3, 2003.
15. Vahabisani, N., S. Khan, and M. Daneshmand, "Microfluidically reconfigurable rectangular waveguide filter using liquid metal posts," *IEEE Microw. and Wiresless Compon. Lett.*, Vol. 10, 801–803, 2016.
16. Macchiarella, G. and S. Tamiazzo, "Design techniques for dual-passband filters," *IEEE Trans. Microw. Theory Tech.*, Vol. 53, No. 11, 3265–3271, Nov. 2005.
17. Amari, S. and M. Bekheit, "A new class of dual mode dual band waveguide filters," *IEEE Trans. Microw. Theory Tech.*, Vol. 56, No. 8, 1938–1944, 2008.
18. Nocella, V., L. Pelliccia, C. Tomassoni, and R. Sorrentino, "Miniaturized dual band waveguide filter using TM dielectric-loaded dual-mode cavities," *IEEE Microw. and Wiresless Compon. Lett.*, Vol. 26, No. 5, 310–312, 2016.
19. Lee, J., M. S. Uhm, and I. B. Yom, "A dual-passband filter of canonical structure for satellite applications," *IEEE Microw. and Wiresless Compon. Lett.*, Vol. 14, No. 6, 310–312, 2004.
20. Bage, A. and S. Das, "Compact triple band waveguide bandpass filter using concentric multiple complementary split ring resonator," *Journal of Circuit System and Computers*, Vol. 26, No. 6, 2017.